Mechanism of coercivity in epitaxial $SmCo_5$ thin films

A. Singh,* V. Neu,† S. Fähler, K. Nenkov, L. Schultz, and B. Holzapfel
IFW Dresden, Institute for Metallic Materials, P.O. Box 270116, D-01171 Dresden, Germany
(Received 6 September 2007; revised manuscript received 6 December 2007; published 28 March 2008)

The magnetization reversal mechanism in pulsed laser deposited, hard magnetic epitaxial $SmCo_5$ thin films with high coercivity (>3 T) and remanent polarization (0.94 T) is investigated. From temperature and angle dependent hysteresis measurements in the framework of the micromagnetic model, we show that the magnetization reversal is described by a hindered domain wall movement. This conclusion from a global analysis is supported by magnetic force microscopy, by imaging the domain evolution in the magnetization process. The smallest stable magnetic entity is found to be of the order of 150 nm. The excessive number of grain boundaries due to the nanometer length scale of the grain size, in addition to possible defects within the grains, is expected to be the key to the excellent magnetic properties and the observed magnetization reversal mechanism.

DOI: 10.1103/PhysRevB.77.104443 PACS number(s): 75.60.Jk, 75.70.Ak, 75.70.Kw, 68.37.Rt

I. INTRODUCTION

Magnetic thin films and heterostructures are getting increasingly popular due to the insatiable demand in magnetic recording, magnetization sensors, and a variety of other applications. In order for the functionality of these systems to be properly exploited, much effort has been made to understand the nucleation and pinning properties of thin films.[1–3] Moreover, due to the high Curie temperature (800 °C), $SmCo_5$ and Sm_2Co_{17} magnets are the favored magnetic materials for high-temperature applications. The magnetization reversal in bulk $SmCo_5$-based magnets is considered to be mainly nucleation controlled,[4,5] whereas Sm_2Co_{17}-based magnets require Cu additions and a complicated thermal processing to obtain a microstructure suitable for domain wall pinning. The detailed pinning mechanism is, however, controversially discussed.[6–9]

Thin film applications benefit from the huge magnetocrystalline anisotropy of $SmCo_5$,[10] which is more than twice as high as that of $L1_0$ ordered phases[11] and, thus enables, e.g., a reduction of the critical grain size for magnetic recording to withstand the superparamagnetic limit. Moreover, the well-defined geometry of hard-soft bilayers,[12,13] trilayers,[14] and multilayers[15,16] makes Sm-Co well suited to study exchange coupling for an enhanced energy product. Both these areas profit from a uniaxial alignment of the easy axis and require sufficiently high coercivities in thin films. Since the maximum obtainable coercivity is strongly dependent on the grain microstructure and domain sizes, a sound knowledge of the smallest magnetic entity becomes unavoidable.

Although a reasonable number of literature is available on the magnetization reversal mechanism of bulk Sm-Co magnets, their thin film counterparts have not been investigated to a similar extent.[17–20] One of the difficulties is the isolation of $SmCo_5$, with the highest uniaxial magnetocrystalline anisotropy of the Sm-Co phases, as a pure phase without any other Sm-Co phases. Another difficulty is the crystallographic growth control for this phase, such that the grains grow in a manner that only one *c*-axis orientation exists throughout the sample. Epitaxial Sm-Co films with well-defined easy axis orientation have been prepared by Fullerton *et al.* [18] with a nominal Sm content of 20 at. % on MgO single crystal substrates by magnetron sputtering. Transmission electron microscopy (TEM) investigations found chemical inhomogeneities within the individual grains in the form of stacking faults, which are discussed as possible pinning centers.[21] To date, no detailed investigation has been reported on the magnetization reversal mechanism of single textured, single phase $SmCo_5$ thin films.

In this work, the $SmCo_5$ phase is prepared as an epitaxial film with a single orientation of the *c*-axis in the film plane and with intrinsic properties (saturation polarization, anisotropy) comparable to single crystal data. This paper clarifies the coercivity mechanism in these well textured $SmCo_5$ thin films by a combination of temperature dependent and angular dependent magnetic measurements in accordance with Kronmüller's modified micromagnetic model[22] and the Kondorsky model,[23] and by direct observation of magnetic domains using field dependent magnetic force microscopy. Differences to bulk Sm-Co and consequences for applications are discussed.

II. EXPERIMENT

Thin $SmCo_5$ films (about 50 nm thickness) were prepared at a temperature of 550 °C on MgO(110) single crystal substrates using pulsed laser deposition (KrF excimer laser, 248 nm, 25 ns) in a UHV chamber (base pressure $\sim 3 \times 10^{-9}$ mbar). Pure Cr films, 10 nm in thickness, were deposited at 400 °C and at a temperature below 150 °C as a buffer and a protecting cover layer, respectively. The choice of the deposition temperature of the Cr buffer is crucial to obtain a high quality hard magnetic film.[24] The intended composition of the $SmCo_5$ film was adjusted by pseudocosputtering from elemental Sm and Co targets with a precalculated number of laser pulses on each target based on individual deposition rates. The resulting composition and film thickness were determined by comparative energy dispersive x-ray (EDX) measurements of film and elemental bulk standards at different electron beam acceleration voltages in combination with a thin film software. Details are given by Neu *et al.*[25] The crystallographic structure and ep-

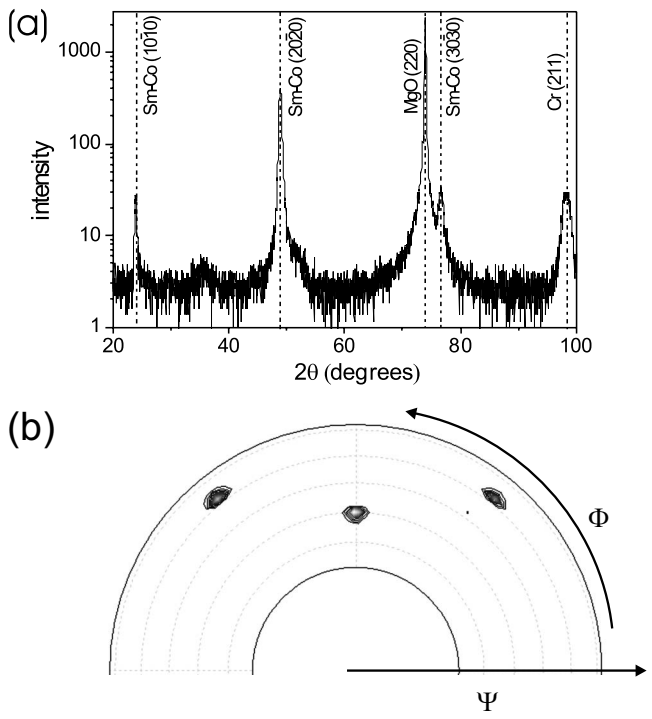

FIG. 1. (a) X-ray diffraction pattern for a (10−10) oriented $SmCo_5$ film deposited on a (211) oriented Cr buffer on a (110) MgO substrate, and (b) $SmCo_5$ (10−11) pole figure demonstrating a single epitaxial orientation with respect to the substrate.

itaxial growth relationships were analyzed by x-ray diffraction using Co $K\alpha$ radiation in Bragg–Brentano geometry and multiple pole figure measurements using Cu $K\alpha$ radiation. The magnetic properties were investigated using a 7 T Quantum Design superconducting quantum interference device magnetometer with sample rotation facility and a physical properties measurement system vibrating sample magnetometer, which operates in fields up to 9 T. Magnetic force microscopy (MFM) measurements were performed in tapping mode with a Digital Instruments Dimension 3100 atomic force microscope equipped with a phase extender box using magnetically coated tips (MFMR by Nanosensors) in a lift height of 60 nm. The images were recorded in the remanent state after applying subsequently higher external magnetic fields. In order to better visualize the in-plane domain structure with the given tip magnetization along the z direction (normal to the film surface), a continuous film has been structured into 10×10 μm^2 sized elements by optical lithography and ion etching.

III. RESULTS AND DISCUSSION

A. Crystallographic and magnetic texture

The x-ray diffractogram [Fig. 1(a)] shows $SmCo_5$ (10−10), (20−20), and (30−30) reflections together with the Cr(211) and MgO(220) reflection of a 50 nm thick $SmCo_5$ film grown on a Cr buffered MgO single crystal substrate, indicating an orientation of the $SmCo_5$ c axes within the substrate plane. Pole figure measurements of the Cr (not shown here) and the $SmCo_5$ layer [Fig. 1(b)] furthermore

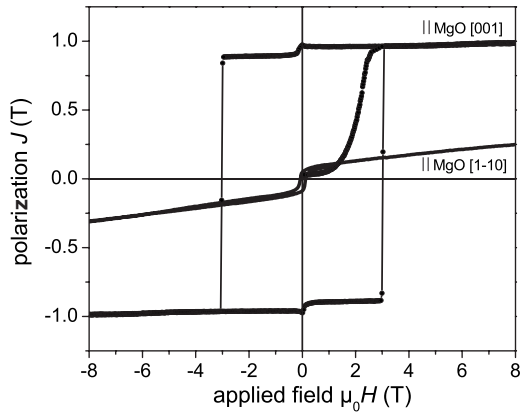

FIG. 2. Magnetic hysteresis of a $SmCo_5$ film measured along the easy magnetization axis (||MgO[001]) and along the in-plane hard axis (||MgO[1−10]).

reveal that the $SmCo_5$ grows epitaxially as per the relationship

$$SmCo_5(10-10)[0001] \parallel Cr(211)[0-11] \parallel MgO(110)[001]$$

with a single orientation of the $SmCo_5$ c axes along an in-plane substrate edge (MgO[001]) and an angular spread of about 5°. The epitaxial relationship observed in TEM for $SmCo_5$ films prepared under similar conditions[24] is thus confirmed by a global texture measurement and is in agreement with the texture observed in sputter deposited Sm_2Co_7 films[18] and hexagonal $PrCo_7$ films.[26] Following the procedure used for films prepared on MgO(100) substrates,[27] multiple pole figure measurements and θ-2θ scans on several tilted poles allow an unambiguous identification of the 1:5 phase. Contrary to highly coercive, epitaxial FePt (Ref. 28) and $Nd_2Fe_{14}B$ (Ref. 29) films, which form isolated grains, the $SmCo_5$ films are continuous and exhibit a typical rms roughness of only 3 nm. First TEM investigations reveal that these films consist of individual grains of about 50–100 nm, connected by small angle grain boundaries,[30] which explains the angular spread observed in the texture measurements.

The room temperature hysteresis (Fig. 2) measured parallel to the crystallographic c axis (along MgO [001]) is open and square shaped with a coercivity $\mu_0 H_c$ of 3.1 T and remanence J_r and saturation polarization J_s (extracted at a field of 9 T) of 0.94 and 0.96 T, respectively, characteristic of a well textured hard magnetic material measured along the easy magnetization direction. The small shoulder at zero field is attributed to the magnetic signal of the sample holder. The initial curve has a very low susceptibility χ_{initial}, which is indicative of an energy barrier that needs to be overcome before magnetization in the sample can reach saturation. The high energy barrier for magnetization increase may arise from the pinning of domain walls in these continuous films. The in-plane hard axis hysteresis (parallel to MgO[1−10] or at 90° to the easy axis) is flat and narrow with no significant coercivity or remanence. The pronounced in-plane magnetic texture ($J_r^{\text{perp}}/J_r^{\text{parallel}}=0.05$) is in agreement with the good crystallographic texture. Hence, along the hard axis, only a reversible rotation of the magnetization is measured. Lin-

early extrapolated easy and hard axis loops intersect at 28 T (not shown here), which is in excellent agreement with the anisotropy field $\mu_0 H_a$ of single crystal $SmCo_5$.[31] The slightly reduced polarization value [J_s (single crystal) ~1.05 T (Ref. 32)] may come from an overestimation of the film thickness or a portion within the film of reduced magnetization often found in thin magnetic samples and denoted as a "dead layer."

B. Micromagnetic analysis

The micromagnetic model[33] defines the coercivity $\mu_0 H_c$ as the reduction in the nucleation field $\mu_0 H_n$ by introducing temperature independent parameters α_{eff} and N_{eff} in the form of the following equation:[34]

$$\mu_0 H_c(T) = \alpha_{\text{eff}} \mu_0 H_n(T) - N_{\text{eff}} J_s(T), \tag{1}$$

where $\mu_0 H_n(T)$ is the theoretical field at which the reversal would take place in case of a defect-free, ellipsoidal, uniaxial single domain particle when the external field is applied along the easy magnetization direction antiparallel to the former saturation. It is determined only by the intrinsic properties of the hard magnetic phase, independent of any microstructural defects. However, in a real magnet with a given (granular) microstructure, the magnetization reversal is modified due to structural or chemical inhomogeneities, grain misalignment, and local stray fields arising from the overall magnetization distribution. These three effects are considered in the parameters α_{eff} and N_{eff}. For this, the parameter α_{eff} is furthermore split up as

$$\alpha_{\text{eff}} = \alpha_K \alpha_\Phi, \tag{2}$$

where α_K incorporates the effect of the sample microstructure, especially inhomogeneities of the intrinsic material parameters, and α_Φ quantifies the easy axis misorientation, and therefore governs the angular dependence of the reversal field in well textured samples. The parameter N_{eff} quantifies magnetostatic interactions and depends as such on grain shape. In an alternative interpretation, an equation of the same mathematical form as Eq. (1) can describe the coercivity of a permanent magnet as controlled by pinning, only that the parameter α_K now characterizes the pinning strength. The absolute value of α_K can provide a distinction between the magnetization reversal mechanisms of coherent rotation and pinning controlled domain wall movement.[35]

To evaluate the above given relation [Eq. (1)], hysteresis loops have been measured along the easy magnetization direction (parallel MgO[001]) in the temperature range from 350 K down to 10 K. For all temperatures, the hysteresis maintains its square shape with a well-defined coercivity. The value of the coercive field increases monotonously with decreasing temperature and is summarized in Fig. 3(a). Furthermore, the magnetization measured at 9 T also increases with decreasing temperature following the known temperature dependence of the saturation magnetization for $SmCo_5$ (solid line) from single crystal measurements[32] but for the already mentioned slightly reduced absolute values.

The nucleation field $\mu_0 H_n$ in $SmCo_5$ is known to be determined by the first anisotropy constant K_1 only and is expressed by $2K_1/J_s$. The temperature dependent values of K_1 are taken from measurements on $SmCo_5$ single crystals.[10] The linear relationship between the normalized coercivity ($\mu_0 H_c/J_s$) and the normalized nucleation field ($\mu_0 H_n/J_s$) expressed by Eq. (1) is graphically displayed in Fig. 3(b). From a linear fit, one obtains $\alpha_{\text{eff}}=0.18\pm0.01$ and $N_{\text{eff}}=3.1\pm0.4$. Unlike the demagnetizing factor N of a homogeneously magnetized sample, which can only obtain values between 0 and 1, the effective demagnetizing factor N_{eff} can reach values above unity when flux is strongly concentrated and local stray fields rise above the saturation magnetization of the magnetic phase. The large value of N_{eff} indicates that, indeed, stray field enhancements at sharp grain edges contribute to a reduced coercivity. The larger effect, however, comes from the value of 0.18 of α_{eff}, which is almost entirely attributable to the microstructural parameter α_K since $\alpha_\Phi \approx 1$ contributes negligibly along the easy axis owing to the very good crystallographic texture in these films. This measured value of α_K is smaller than the critical value of 0.35, which clearly demarcates nucleation (existing at $\alpha_K > 0.35$) from a regime where both nucleation and pinning controlled magnetization reversal coexist ($\alpha_K < 0.35$).[35]

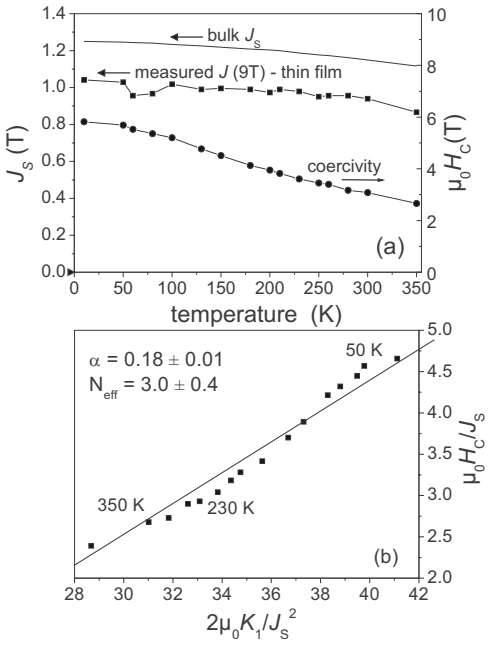

FIG. 3. (a) Polarization at 9 T (solid squares), coercivity (solid circles), and saturation polarization (solid line) of $SmCo_5$ single crystal (after 32) vs temperature, and (b) analysis of the data according to the normalized equation (1) (solid symbols), showing a good linear fit with a slope of 0.18.

Further information on the coercivity mechanism can be obtained from angle dependent hysteresis measurements, where the external field is applied at a certain angle θ with respect to the easy axis of the sample. Such measurements are presented in Fig. 4, with the field rotating from the in-plane easy axis ($\theta=0°$) toward the in-plane hard axis ($\theta=90°$). The hysteresis measured along the easy axis is perfectly square shaped and the entire sample switches its magnetization irreversibly at one applied field value in a very narrow field range, as already shown in Fig. 2. The hysteresis

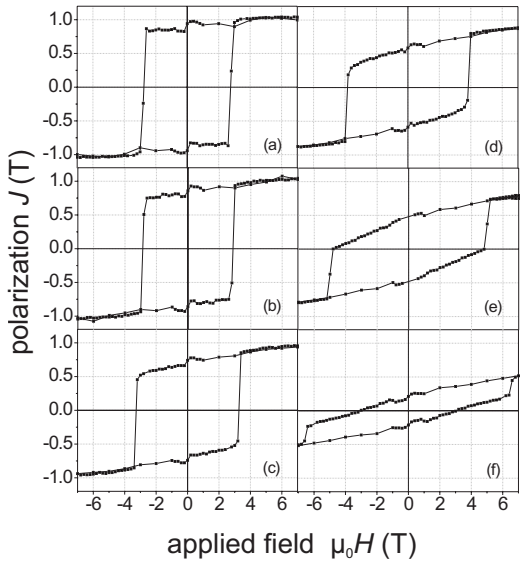

FIG. 4. Room temperature magnetic hystereses of a $SmCo_5$ film measured at varying angles between the easy axis and the applied field. [(a)–(f)] Hysteresis measurements for 0°, 20°, 40°, 60°, and 70°, respectively. At measurement angles larger than 50°, the coercivity is clearly different from the switching field.

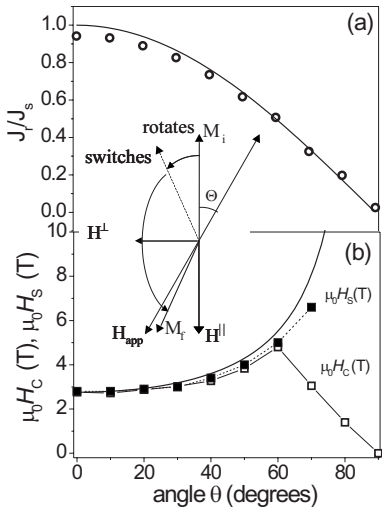

FIG. 5. (a) Normalized remanent polarization J_r/J_s as a function of the angle θ (open symbols) together with the expected cos θ behavior (solid line). (b) Angular variation of switching field $\mu_0 H_{SW}$ (solid symbols) and coercivity $\mu_0 H_c$ (open symbols) together with an inverse cos θ curve (continuous line). Inset: Measurement configuration illustrating the demagnetizing process. The perpendicular field component $H^{\perp}=H_{perp}=H_{app}$ sin θ causes a rotation of the magnetization away from the easy axis, whereas the parallel component $H^{\parallel}=H_{eff}=H_{app}$ cos θ is responsible for the irreversible switching.

gradually changes in shape with increasing angle θ. The slope of the demagnetizing branch increases at higher measurement angles, indicating that the magnetization first rotates toward the field direction before it switches irreversibly. The remanent magnetization J_r decreases with increasing angle θ [Fig. 5(a)]. Since the magnetization in the remanent state lies along the easy axis, one measures only the projection of J_s along the field direction and thus expects an angle dependence according to

$$J_r = J_s \cos\,\theta, \tag{3}$$

which perfectly fits the experimental data. For an analysis of magnetization reversal, the coercivity $\mu_0 H_c$ has to be distinguished from the switching field $\mu_0 H_{sw}$. The coercivity is the field required to bring the magnetization to zero and, hence has contributions from reversible rotation and irreversible switching. The switching field, on the other hand, describes only irreversible processes and is defined as the maximum of the irreversible susceptibility. From recoil loop measurements (to be published elsewhere), the irreversible and the total susceptibilities are found to be very similar, so that the switching field has been deduced with high accuracy from the field derivative of the measured hysteresis. Figure 5(b) summarizes the switching fields and coercivities obtained in the angular dependent hysteresis measurements. Both the coercivity and the switching field increase up to measurement angles of 60°; thereafter, the coercivity drops to zero on approaching θ=90°, whereas the switching field continues to increase. The difference between $\mu_0 H_c$ and $\mu_0 H_{sw}$ is clearly seen for the hysteresis at θ=70° in Fig. 4(f). For angles larger than 70°, the available field of 7 T was not sufficient to switch the magnetization. The measured data points follow an inverse cos θ curve (shown as solid line), suggested by Kondorsky[23] for uniaxial (such that only 180° domain walls are present) highly anisotropic systems (such that $\mu_0 H_a \gg \mu_0 H_c$), indicating a magnetization reversal that is dominated by depinning of domain walls. The magnetization thus reverses when the effective field H_{eff} parallel to the easy axis overcomes the switching field established at 0°, i.e.,

$$H_{eff}(\theta) = H_{app} \cos\,\theta = H_{sw}(0\,^{\circ}). \tag{4}$$

The inverse cos θ dependence was observed previously in highly anisotropic but low coercive single crystals,[36–39] soft magnetic films,[40,41] and also sintered $SmCo_5$ bulk magnets.[42] The observed angle dependency is in clear discrepancy to the nucleation process typically considered in the micromagnetic model, which is based on a coherent rotation process in an area with reduced anisotropy.[22] On the other hand, the already mentioned depinning of a 180° wall would fully explain the observed experimental behavior. However, one has to be cautious in drawing the reverse conclusion. Givord *et al.*[42] pointed out that a thermally activated magnetization reversal process in a coarse grained uniaxial magnet, which necessarily has to start with the creation of a domain wall, should generally lead to a similar angle dependency. In this phenomenological approach, details on the exact coercivity mechanism cannot be drawn.

Irrespective of this open question, the agreement of the measured angular dependent switching field as close to the theoretically predicted $1/\cos\,\theta$ law for an ideal uniaxial system vouches for the high texture quality of these epitaxial samples and was not yet reported before for a hard magnetic film. If interpreted as a pinning dominated reversal mechanism, the large coercivity in these thin films suggests a very

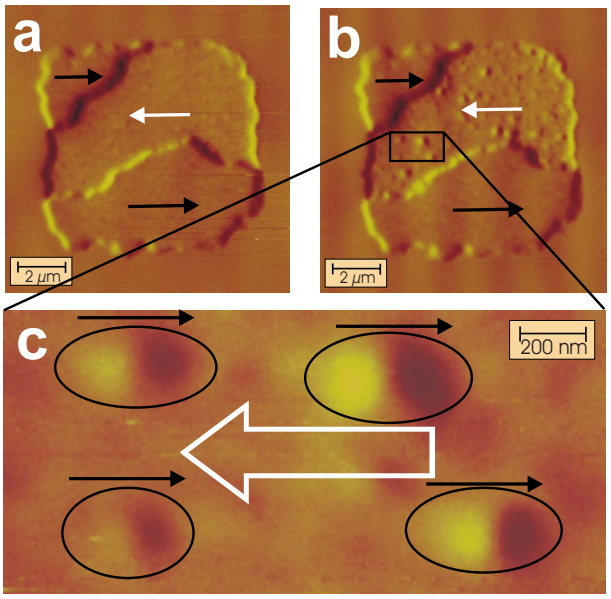

FIG. 6. (Color online) (a) MFM structure of a patterned $SmCo_5$ element not affected by a magnetic field, which remains unaltered in the remanent state after applying successively higher fields up to 1.8 T. (b) First occurrence of magnetization switching at 2 T. (c) High magnification measurement of the framed area showing small individual reversed areas within the large, oppositely oriented domain.

good pinning of the domain walls at various inhomogeneities in the sample.

C. Magnetic force microscopy

In order to access the magnetic domain structure and the domain evolution upon applying an external field, MFM measurements have been performed on a structured $SmCo_5$ film. In the as-prepared state, the continuous film possesses large, micrometer-sized domains with the magnetization oriented in both possible directions allowed by the easy axis,[25] which results in a likewise coarse domain structure when the film is patterned. Figure 6(a) displays a structured element with three clearly visible domains. As expected from the in-plane magnetization and the fact that the MFM measurement is only sensitive to gradients of the z component of the stray field, the domains are not distinguished by a different area contrast but rather by stray fields emerging from the domain boundaries, such as the domain walls and the element borders. The observed domain structure is completely unaltered up to an applied field of 1.8 T. When a field of 2 T is applied in the positive x direction, irreversible magnetization processes are identified by the contrast change within the large domain pointing in the negative x direction [Fig. 6(b)]. It is apparent that the magnetization process does not occur via the movement of the already existing domain wall but via nucleation and hindered expansion of new domains, and can be thus named a pinning dominated mechanism. A very similar behavior has been observed in fine grained $SmCo_5$ films grown epitaxially on MgO(100) substrates,[43] however with the difference that those samples consist of two subsets of grains with perpendicular orientation of their c axes and that the initial magnetization state consisted of a very small scaled domain structure. The magnification of the framed area [Fig. 6(c)] of Fig. 6(b) shows the stray field contrast of the small magnetic objects on a length scale of 200–300 nm. Four of them are encircled in Fig. 6(c) and some more of them can be identified by careful investigation of the images, but in none of the cases was their size significantly below 200 nm, although the lateral resolution of MFM is capable of detecting isolated magnetic objects as small as 50 nm. Independent of the details of the contrast mechanism, the size of the underlying domain can be estimated from the distance between phase shift minimum and maximum within the magnetic object. This leads to a size of 150–200 nm for the typically observed isolated magnetic domains. With this clear demonstration of a pinning behavior, the strong pinning sites, which determine coercivity by blocking the domain expansion even up to fields of 2 T, therefore have a likewise average distance of the order of 150–200 nm. Weaker pinning sites may exist on a smaller length scale, but they do not hinder domain wall movement sufficiently to contribute to the coercivity mechanism.

IV. CONCLUSIONS

In conclusion, this paper reports on the analysis of the magnetization reversal mechanism in single textured epitaxial $SmCo_5$ thin films. The low initial susceptibility, the low microstructural parameter K_α obtained by micromagnetic analysis, the $1/\cos\theta$ angular dependence of the switching field, and, finally, the direct observation of a magnetization process by MFM show that the large coercivity of 3.1 T in these epitaxial $SmCo_5$ films is obtained by pinning of domain walls. This is contrary to nucleation controlled $SmCo_5$ bulk magnets but also presents a different pinning mechanism in comparison to Sm_2Co_{17}-based magnets, where the pinning is caused by local anisotropy variations introduced by Cu additions and a complex heat treatment. The magnetic force microscopy images reveal that magnetic domains in these epitaxial films are as small as 150 nm, which indicates a high density of pinning sites. Although x-ray diffraction measurements only show the pure 1:5 phase, the low deposition temperatures may introduce defects such as stacking faults, which may act as additional, weaker pinning centers. The domain scale compares well with the average grain size of 50–100 nm, giving rise to the surprising but important explanation that even small angle grain boundaries present in the epitaxial films represent effective pinning centers. The pinning-type character makes the coercivity inherently more robust against defects occurring due to oxidation[44] or patterning.[3,45] Thus, these smooth, continuous $SmCo_5$ films are especially suitable for microstructured devices.

ACKNOWLEDGMENTS

The authors would like to acknowledge financial support of DFG via SFB 463, "Rare Earth Transition Metal Compounds—Structure, Magnetism and Transport," and I. Mönch for patterning of the $SmCo_5$ films.

*Present address: Los Alamos National Laboratory, Neutron Scattering Center, Los Alamos, NM 87545; asingh@lanl.gov
†Corresponding author: v.neu@ifw-dresden.de

[1] Y. Pennec, J. Camarero, J. C. Toussaint, S. Pizzini, M. Bonfim, F. Petroff, W. Kuch, F. Offi, K. Fukumoto, F. Nguyen Van Dau, and J. Vogel, Phys. Rev. B **69**, 180402(R) (2004).
[2] K. Fukumoto, W. Kuch, J. Vogel, F. Romanens, S. Pizzini, J. Camarero, M. Bonfim, and J. Kirschner, Phys. Rev. Lett. **96**, 097204 (2006).
[3] T. Thomson, G. Hu, and B. D. Terris, Phys. Rev. Lett. **96**, 257204 (2006).
[4] W. Sattler and E. Adler, J. Magn. Magn. Mater. **15-18**, 1447 (1980).
[5] K. J. Strnat, D. Li, and H. F. Mildrum, J. Appl. Phys. **55**, 2100 (1984).
[6] Y. Zhang, A. Gabay, Y. Wang, and G. Hadjipanayis, J. Magn. Magn. Mater. **272-276**, e1899 (2004).
[7] J. Fidler, T. Schrefl, S. Hoefinger, and M. Hajduga, J. Phys.: Condens. Matter **16**, S455 (2004).
[8] D. Goll, H. Kronmüller, and H. H. Stadelmaier, J. Appl. Phys. **96**, 6534 (2004).
[9] A. Yan, A. Handstein, T. Gemming, K.-H. Müller, and O. Gutfleisch, J. Magn. Magn. Mater. **290**, 1206 (2005).
[10] B. Barbara and M. Uehara, IEEE Trans. Magn. **12**, 997 (1976).
[11] T. Klemmer, D. Hoydick, H. Okumura, B. Zhang, and W. A. Soffa, Scr. Metall. Mater. **33**, 1793 (1995).
[12] E. E. Fullerton, J. S. Jiang, M. Grimsditch, C. H. Sowers, and S. D. Bader, Phys. Rev. B **58**, 12193 (1998).
[13] V. K. Vlasko-Vlasov, U. Welp, J. S. Jiang, D. J. Miller, G. W. Crabtree, and S. D. Bader, Phys. Rev. Lett. **86**, 4386 (2001).
[14] V. Neu, K. Häfner, A. K. Patra, and L. Schultz, J. Phys. D: Appl. Phys. **39**, 5116 (2006).
[15] S. Wüchner, J. C. Toussaint, and J. Voiron, Phys. Rev. B **55**, 11576 (1997).
[16] J. Zhang, Y. K. Takahashi, R. Gopalan, and K. Hono, Appl. Phys. Lett. **86**, 122509 (2005).
[17] F. J. Cadieu, T. D. Cheung, L. Wichramasekara, N. Kamprath, H. Hegde, and N. C. Liu, J. Appl. Phys. **62**, 3866 (1987).
[18] E. E. Fullerton, J. S. Jiang, C. Rehm, C. H. Sowers, S. D. Bader, J. B. Patel, and X. Z. Wu, Appl. Phys. Lett. **71**, 1579 (1997).
[19] C. Prados, A. Hernando, G. C. Hadjipanayis, and J. M. Gonzales, J. Appl. Phys. **85**, 6148 (1999).
[20] E. Pina, M. A. García, I. Carabias, F. J. Palomares, F. Cebollada, A. de Hoyos, R. Almazan, M. I. Verdú, M. T. Montojo, G. Vergara, A. Hernando, and J. M. González, J. Magn. Magn. Mater. **272-276**, 2833 (2004).
[21] M. Benaissa, K. M. Krishnana, E. E. Fullerton, and J. S. Jiang, IEEE Trans. Magn. **34**, 1204 (1998).
[22] H. Kronmüller, Phys. Status Solidi B **130**, 197 (1985).
[23] E. Kondorsky, J. Phys. (USSR) **2**, 161 (1940).
[24] A. Singh, V. Neu, R. Tamm, K. Subba Rao, S. Fähler, W. Skrotzki, L. Schultz, and B. Holzapfel, J. Appl. Phys. **99**, 08E917 (2006).
[25] V. Neu, S. Fähler, A. Singh, A. R. Kwon, A. K. Patra, U. Wolff, K. Häfner, B. Holzapfel, and L. Schultz, J. Iron Steel Res. Int. **13**, 102 (2006).
[26] A. K. Patra, V. Neu, S. Fähler, R. Groetzschel, and L. Schultz, Appl. Phys. Lett. **89**, 142512 (2006).
[27] A. Singh, V. Neu, R. Tamm, K. Rao, S. Fähler, W. Skrotzki, L. Schultz, and B. Holzapfel, Appl. Phys. Lett. **87**, 072505 (2005).
[28] M. Weisheit, L. Schultz, and S. Fähler, J. Appl. Phys. **95**, 7489 (2004).
[29] V. Neu, S. Melcher, U. Hannemann, S. Fähler, and L. Schultz, Phys. Rev. B **70**, 144418 (2004).
[30] K. Subba Rao, doctorals thesis, Dresden University of Technology, 2006.
[31] H. R. Kirchmayr, J. Phys. D **29**, 2763 (1996).
[32] H. P. Klein, A. Menth, and R. S. Perkins, Physica B & C **80**, 153 (1975).
[33] W. F. Brown, Rev. Mod. Phys. **17**, 15 (1945).
[34] H. Kronmüller, K.-D. Durst, and G. Martinek, J. Magn. Magn. Mater. **69**, 149 (1987).
[35] H. Kronmüller, K.-D. Durst, and M. Sagawa, J. Magn. Magn. Mater. **74**, 291 (1988).
[36] S. Reich, S. Shtrikman, and D. Treves, J. Appl. Phys. **36**, 140 (1965).
[37] J. J. Becker (AIP Conference Proceedings), Vol. 5, p. 1067, 1972.
[38] A. Menth, H. P. Klein, J. Bernasconi, and S. Strässler, AIP Conf. Proc. **18**, 1182 (1974).
[39] A. S. Ermolenko, IEEE Trans. Magn. **12**, 992 (1976).
[40] F. Y. Yang, C. L. Chein, E. F. Ferrari, X. W. Li, G. Xiao, and A. Gupta, Appl. Phys. Lett. **77**, 286 (2000).
[41] Z.-H. Wang, G. Cristiani, and H.-U. Habermeier, Appl. Phys. Lett. **82**, 3731 (2003).
[42] D. Givord, P. Tenaud, and T. Viadieu, J. Magn. Magn. Mater. **72**, 247 (1988).
[43] U. Wolff, A. Singh, L. Schultz, and V. Neu, J. Magn. Magn. Mater. **310**, 2210 (2007).
[44] S. Fähler, U. Hannemann, S. Oswald, V. Neu, B. Holzapfel, and L. Schultz, IEEE Trans. Magn. **39**, 2950 (2003).
[45] B. D. Terris and T. Thomson, J. Phys. D: Appl. Phys. **38**, R199 (2005).